

Structure and magnetic properties of nanocrystalline $(\text{Fe}_{1-x}\text{Co}_x)_{90}\text{Zr}_7\text{B}_2\text{Cu}_1$ ($0 \leq x \leq 0.6$)

T. Kemény,^{a)} D. Kaptás, L. F. Kiss, J. Balogh, and L. Bujdosó
Research Institute for Solid State Physics and Optics, H-1525 Budapest, Hungary

J. Gubicza and T. Ungár
Department of General Physics, Eötvös University, H-1518 Budapest, Hungary

I. Vincze
*Research Institute for Solid State Physics and Optics, H-1525 Budapest, Hungary
 and Department of General Physics, Eötvös University, H-1518 Budapest, Hungary*

(Received 6 October 1999; accepted for publication 16 February 2000)

Nanocrystalline $(\text{Fe}_{1-x}\text{Co}_x)_{90}\text{Zr}_7\text{B}_2\text{Cu}_1$ ($0 \leq x \leq 0.6$) alloys were investigated by x-ray diffraction, ^{57}Fe Mössbauer spectroscopy, and magnetic measurements. The grain size did not change significantly with composition. Co was preferentially partitioned to the residual amorphous phase, and the bcc grains were accordingly enriched by Fe. The room-temperature coercive field increased with the Co addition, which is attributed to the increasing magnetostriction constant. © 2000 American Institute of Physics. [S0003-6951(00)03215-0]

The nanocrystalline (nc) Fe–M–B(Cu) alloys¹ (where M is an early transition metal such as Zr, Nb, etc.) and the formerly discovered ncFe–Nb–Si–B(Cu) alloys² (i.e., FINEMET) show superior soft-magnetic properties (high initial permeability together with a substantial saturation magnetization). These nanocrystalline alloys are prepared by partial crystallization of amorphous ribbons resulting in nanosize crystalline bcc precipitates in a residual amorphous matrix. The explanation of the good soft-magnetic properties is of both fundamental and technical interest and at present it is a controversial issue. It is generally acknowledged that the reduction of the effective magnetocrystalline anisotropy on forming ultrafine grains plays a decisive role. Since the observation that in ncFe–Nb–Si–B(Cu) alloys the good soft-magnetic properties show a fast deterioration above the Curie temperature T_c , of the ferromagnetic residual amorphous phase, the important role of the connecting tissue in the coupling of the ferromagnetic bcc grains is implied.²

Recently, a class of nanocrystalline alloys with composition $\text{Fe}_{44}\text{Co}_{44}\text{Zr}_7\text{B}_4\text{Cu}_1$ has been developed,^{3,4} which are capable of operating at higher temperatures and have good soft-magnetic properties. They are promising as high-temperature magnetic applications, e.g., as rotors in electric aircraft. Here, we report a systematic study of slightly different composition nanocrystalline alloys with higher Fe–Co content and, consequently, with higher saturation magnetization, which is one of the key intrinsic magnetic properties.

Amorphous nc $(\text{Fe}_{1-x}\text{Co}_x)_{90}\text{Zr}_7\text{B}_2\text{Cu}_1$ ($0 \leq x \leq 0.6$) ribbons were melt spun in protective atmosphere. The samples were heat treated in a Perkin-Elmer differential scanning calorimeter with a 20 K/min heating rate until the end of the first crystallization stage, well resolved between 820 and 870 K for the different samples. Due to the marked separation of the two crystallization stages, 20 K changes in heat treatment temperature yielded identical nanocrystalline samples within

our experimental resolution. The transformation heat was independent of Co composition (about 120 ± 10 J/g), which indicates that the amount of the remaining amorphous phase did not change significantly with composition.

The nanocrystalline state of the alloys and the phase of the crystalline grains were identified by x-ray diffraction using a Philips X'pert diffractometer and Cu $K\alpha$ radiation ($\lambda = 0.15418$ nm). The grain size of the bcc Fe–Co granules were determined from the x-ray diffraction profiles [Fig. 1(a)]. The lattice parameters determined from the positions and the average particle sizes obtained from the full widths at half maximum of these profiles by the modified Williamson–Hall procedure^{5,6} are shown in Figs. 1(b) and 1(c). The grain size is between 20 and 30 nm for each composition and the lattice parameter follows the well-known composition trend⁷ of bulk bcc Fe–Co alloys.

^{57}Fe Mössbauer spectroscopy measurements were performed between 12 K and room temperature in a standard-flow cryostat using a conventional constant-acceleration spectrometer with a 50 mCi $^{57}\text{CoRh}$ source at room temperature. The magnetic measurements were performed by a Quantum Design superconducting quantum interference device magnetometer of the type MPMS-5S with a maximum field of 5 T. About five ribbon pieces were fixed with silicon grease on a Si plate, the magnetic field being parallel to the ribbon length.

In Fig. 2 typical Mössbauer spectra measured at 12 K are shown. They have two characteristic features: a relatively narrow sextet with asymmetric shoulders (which is somewhat broadened with increasing Co content), and will be attributed to the bcc granules, and a broad magnetic component belonging to the residual amorphous phase.⁸ The low-temperature Mössbauer parameters [Fig. 3: average isomer shift (IS) and hyperfine field B_m] of the stronger component of the asymmetric sextet, which will be referred to as the main line, are similar to those of bulk bcc Fe–Co alloys.^{9,10} The hyperfine field of the broad shoulder on the low-field

^{a)}Electronic mail: kemeny@power.szfi.kfki.hu

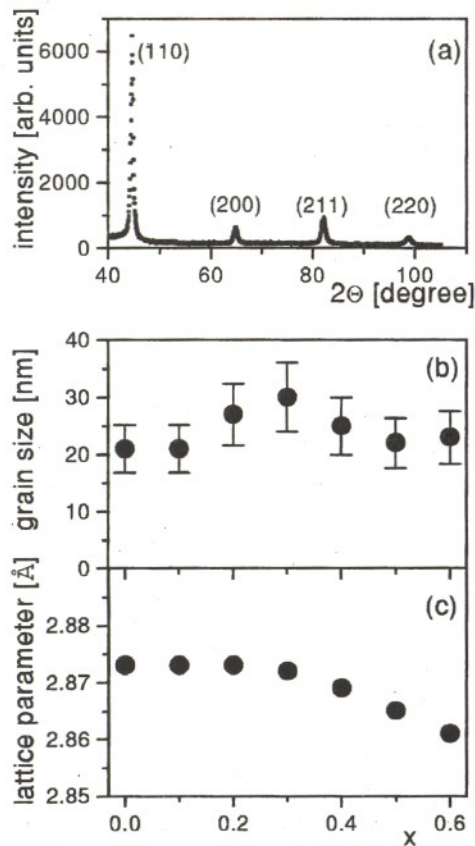


FIG. 1. X-ray powder diffractogram of $ncFe_{72}Co_{18}Zr_7B_2Cu_1$ (a), the composition dependence of the grain size (b), and the lattice parameter of the nanocrystalline Fe-Co particles (c) in $nc(Fe_{1-x}Co_x)_{90}Zr_7B_2Cu_1$.

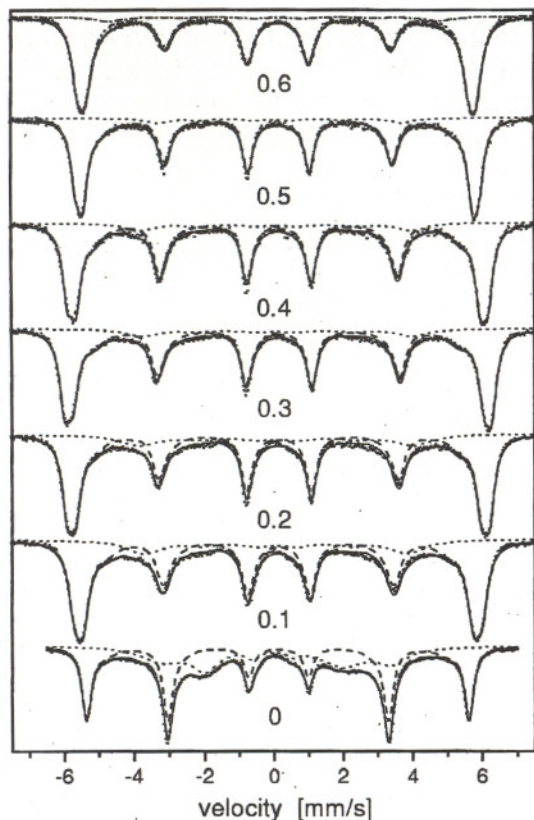


FIG. 2. Mössbauer spectra of $nc(Fe_{1-x}Co_x)_{90}Zr_7B_2Cu_1$ taken at 12 K. The full lines are the fitted curves, the bcc nanocrystalline component (broken line) and the residual amorphous part (dotted line) are marked, respectively. The bcc component has two contributions as shown in the upper part of the figure for $x=0.6$: the main lines (dashed line) and the satellite, i.e., the shoulder lines (dash-dot line), are shown.

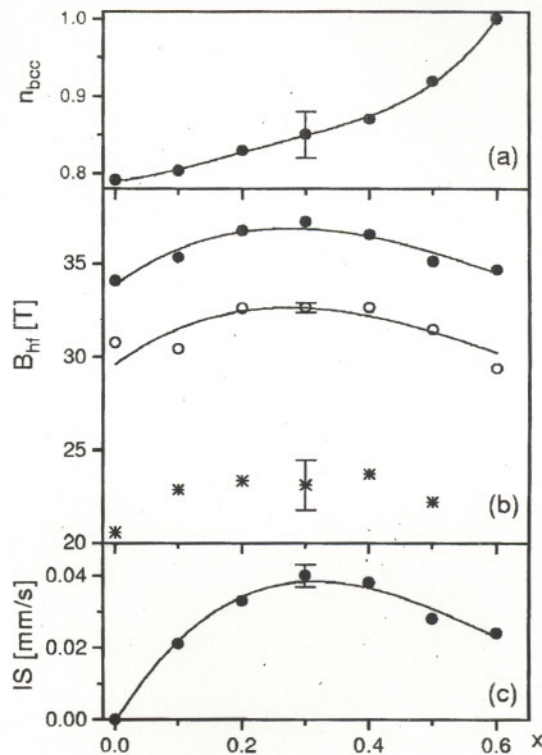


FIG. 3. Composition dependence of the relative number of Fe atoms in the bcc granules, n_{bcc} (a), the average Fe hyperfine field of the main (dots) and shoulder (circles) components of the bcc grains and that of the residual amorphous phase (stars) at 12K (b) and the average isomer shift IS of the main bcc component with respect to that of α -Fe (c), respectively. Typical error bars are shown when they are larger than the applied symbols. The lines are guides to the eye.

side B_s follows this trend. A similar shoulder is often attributed¹¹ to an interfacial phase in $ncFe-Zr-B(Cu)$ -type materials. However, the present composition dependence of B_s supports our former observations⁸ that the nanocrystalline Fe-based bcc phase contains a few percentages of dissolved Zr and B. Thus, B_m is the hyperfine field of Fe atoms with no Zr or B nearest and next-nearest neighbors and B_s is the average hyperfine field of Fe atoms with at least one impurity neighbor in the first two coordination shells.

The relative amount of Fe in the main and in the shoulder component is n_m and n_s , respectively. The Co composition dependence of the fraction of the Fe atoms that are in the bcc phase, $n_{bcc} = n_m + n_s$ is shown in Fig. 3(a). It shows a monotonous increase with increasing Co concentration. At the highest investigated composition, $x=0.6$, no Fe is found in the residual amorphous phase, the respective lines are missing in the spectrum of Fig. 2. This means that the Fe content of the grains is enhanced during nanocrystallization, Co prefers the residual amorphous phase presumably due to the stronger Co-B and Co-Zr than the corresponding Fe-B and Fe-Zr chemical interactions.

The residual amorphous phase is characterized by a hyperfine field distribution; its average hyperfine field B_a is shown in Fig. 3(b). For Co addition, the average magnetic moment of Fe atoms in the residual amorphous phase remains constant within the 10% systematic error limit. The highest Curie temperature of the residual amorphous phase is expected for $x=0.3$ as extrapolated from the room-temperature hyperfine fields.

The composition dependence of the saturation magneti-

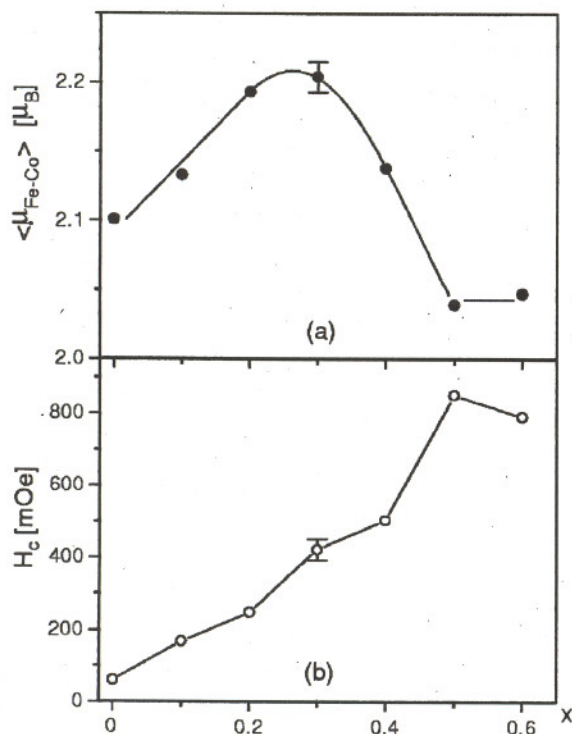


FIG. 4. Composition dependence of the average Fe–Co magnetic moment ($\mu_{\text{Fe-Co}}$) at 12 K (a) and the coercive field at room temperature (b), respectively, in $\text{nc}(\text{Fe}_{1-x}\text{Co}_x)_{90}\text{Zr}_7\text{B}_2\text{Cu}_1$.

zation is shown in Fig. 4(a). It is an average quantity of the magnetic atoms (Fe and Co) in both the nanocrystalline and the residual amorphous phase. Though it follows the well-known trend of bulk Fe–Co alloys, the slightly reduced values indicate the contribution of the residual amorphous phase with smaller atomic moments. Deviation from the bulk trend at $x=0.6$ may indicate ordering of Fe and Co atoms in the nanocrystalline bcc phase as observed formerly in Ref. 4. Our Mössbauer data are not sensitive to such order due to the strongly overlapping spectrum components.

The composition dependence of the coercive field measured at room temperature is shown in Fig. 4(b). A similar increase of the coercive field was observed¹² in Co-substituted FINEMET alloys (FeCoSiBCuNb). The coercive

field is primarily determined by the magnetocrystalline and magnetoelastic anisotropy. The magnetocrystalline anisotropy in bulk Fe–Co alloys decreases¹³ up to 60 at. % Co content. On the other hand, the magnetostriction constant for these alloys increases¹³ with the Co content up to 50 at. %. The magnetic anisotropy field for Fe–Co-evaporated thin films increases with increasing Co content up to 60 at. % followed by a decrease for higher Co compositions.¹⁴ Therefore, the increase of coercivity with Co concentration observed in our samples might be associated with the increasing magnetostriction constant. In our samples the largest saturation magnetization with modest increase of the coercive field was found for concentrations between $\text{Fe}_{72}\text{Co}_{18}\text{Zr}_7\text{B}_2\text{Cu}_1$ and $\text{Fe}_{63}\text{Co}_{27}\text{Zr}_7\text{B}_2\text{Cu}_1$, and the Curie point of the residual amorphous phase is estimated to be the highest for this latter composition, which seems to be optimal for high-temperature soft-magnetic applications.^{3,4}

This work was supported by the Hungarian Research Fund (OTKA T-030753 and D-29339) and by the Hungarian Academy (AKP 98-25 2,2).

- ¹ K. Suzuki, A. Makino, A. Inoue, and T. Masumoto, *J. Appl. Phys.* **70**, 6232 (1991).
- ² G. Herzer, in *Nanomagnetism*, edited by A. Hernando (Kluwer Academic, Dordrecht, The Netherlands, 1993), p. 111; *Scripta Met.* **33**, 1741 (1995).
- ³ M. A. Willard, D. E. Laughlin, M. E. McHenry, D. Thoma, K. Sickafus, J. O. Cross, and V. G. Harris, *J. Appl. Phys.* **84**, 6773 (1998).
- ⁴ M. A. Willard, M.-Q. Huang, D. E. Laughlin, M. E. McHenry, J. O. Cross, V. G. Harris, and C. Franchetti, *J. Appl. Phys.* **85**, 4421 (1999).
- ⁵ T. Ungár and A. Borbély, *Appl. Phys. Lett.* **69**, 3173 (1996).
- ⁶ T. Ungár, S. Ott, P. Sanders, A. Borbély, and J. R. Weertman, *Acta Mater.* **46**, 3693 (1998).
- ⁷ W. C. Ellis and E. S. Greiner, *Trans. Am. Soc. Met.* **29**, 415 (1941).
- ⁸ T. Kemény, D. Kaptás, J. Balogh, L. F. Kiss, T. Pusztai, and I. Vincze, *J. Phys.: Condens. Matter* **11**, 2841 (1999).
- ⁹ B. de Mayo, D. W. Forester, and S. Spooner, *J. Appl. Phys.* **41**, 1319 (1970).
- ¹⁰ I. Vincze, I. A. Campbell, and A. J. Meyer, *Solid State Commun.* **15**, 1495 (1974).
- ¹¹ M. Miglierini and J. M. Greneche, *J. Phys.: Condens. Matter* **9**, 2303 (1997); **9**, 2321 (1997).
- ¹² L. Pascual, C. Gómez-Polo, P. Marín, M. Vázquez, and H. A. Davies, *J. Magn. Magn. Mater.* **203**, 79 (1999).
- ¹³ R. C. Hall, *J. Appl. Phys.* **31**, 157S (1960).
- ¹⁴ C. H. Wiltz and F. B. Humphrey, *J. Appl. Phys.* **39**, 1191 (1968).